diaPASEF Analysis for HLA-I Peptides Enables Quantification of Common Cancer Neoantigens

Authors

Denys Oliinyk, Hem R. Gurung, Zhenru Zhou, Kristin Leskoske, Christopher M. Rose, and Susan Klaeger

Correspondence

klaeger.susan@gene.com

In brief

Here, we evaluate the performance of data-independent acquisition (DIA) in combination with ion mobility (diaPASEF). We generate human leukocyte antigen (HLA) binder-specific *in silico* predicted spectral libraries to further increase the number of identified HLA-I peptides. We applied SILAC-DIA to a mixture of labeled HLA-I peptides and demonstrated that diaPASEF achieves high quantitative accuracy up to 5-fold dilution. The sensitivity and quantitative precision provided by DIA can enable the detection and quantification of less abundant peptide species, such as neoantigens across samples from the same background.

Graphical Abstract

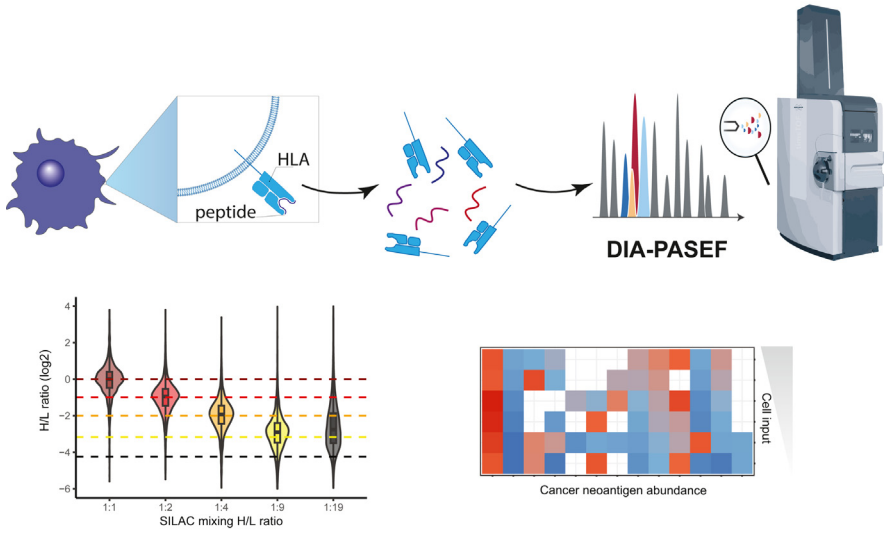

Highlights

- diaPASEF for human leukocyte antigen class I (HLA-I) peptides increases peptidome coverage for low sample amounts.
- HLA binder-specific *in silico* libraries further increased number of HLA-I peptides.
- High quantitative accuracy up to 5-fold dilution in a SILAC-DIA experiment.
- Identification and quantification of cancer neoantigens as low as 1 million cells.

2025, Mol Cell Proteomics *24*(*4*), 100938

https://doi.org/10.1016/j.mcpro.2025.100938

diaPASEF Analysis for HLA-I Peptides Enables Quantification of Common Cancer Neoantigens

Denys Oliinyk[1,2], Hem R. Gurung[1], Zhenru Zhou[1], Kristin Leskoske[1], Christopher M. Rose[1], and Susan Klaeger[1,*]

Human leukocyte antigen class I (HLA-I) molecules present short peptide sequences from endogenous or foreign proteins to cytotoxic T cells. The low abundance of HLA-I peptides poses significant technical challenges for their identification and accurate quantification. While mass spectrometry is currently a method of choice for direct system-wide identification of cellular immunopeptidomes, there is still a need for enhanced sensitivity in detecting and quantifying tumor-specific epitopes. As gas phase separation in data-dependent MS data acquisition increased HLA-I peptide detection by up to 50%, here, we aimed to evaluate the performance of data-independent acquisition (DIA) in combination with parallel accumulation serial fragmentation ion mobility (diaPASEF) for high-sensitivity identification of HLA presented peptides. Our streamlined diaPASEF workflow enabled identification of 11,412 unique peptides from 12.5 million A375 cells and 3426 8-11mers from as low as 500,000 cells with high reproducibility. By taking advantage of HLA binder-specific *in silico* predicted spectral libraries, we were able to further increase the number of identified HLA-I peptides. We applied SILAC-DIA to a mixture of labeled HLA-I peptides, calculated heavy-to-light ratios for 7742 peptides across five conditions and demonstrated that diaPASEF achieves high quantitative accuracy up to 5-fold dilution. Finally, we identified and quantified shared neoantigens in a monoallelic C1R cell line model. By spiking in heavy synthetic peptides, we verified the identification of the peptide sequences and calculated relative abundances for 13 neoantigens. Taken together, diaPASEF analysis workflows for HLA-I peptides can increase the peptidome coverage for lower sample amounts. The sensitivity and quantitative precision provided by DIA can enable the detection and quantification of less abundant peptide species such as neoantigens across samples from the same background.

Sensitive mass spectrometry (MS) methods have greatly advanced the discovery of peptides presented by major histocompatibility complex or human leukocyte antigen (HLA) molecules and helped to inform cancer immunotherapies ((1–3)). However, low abundance, poor recovery yields, and lack of clear digestion rules pose significant challenges for efficient identification of HLA-I peptidome.

As of today, data-dependent acquisition (DDA) remains a method of choice for MS-based immunopeptidomics. High quality of acquired MS/MS spectra obtained in DDA mode can be readily translated into high confidence determination of peptide sequences that makes DDA ideal for discovery immunopeptidomics. Nevertheless, DDA inherently suffers from stochastic intensity-based selection of precursor ions that often leads to low sensitivity and low data completeness. Data-independent acquisition (DIA), in contrast to DDA, employs fragmentation of all precursor ions that fall into predefined mass windows, generating highly complex fragment spectra. Fragmentation of all available precursor ions without prior selection significantly enhances sensitivity and data completeness of an analysis. In recent years, DIA has proven to be an attractive acquisition method for label-free quantification in global proteomics. Analysis of highly complex DIA fragment spectra is a nontrivial task, which traditionally employs time and resource intensive DDA-based spectral libraries. Development and rapid evolution of advanced computational tools enabled an accurate prediction of peptide retention time (RT), ion mobility, and fragment ion intensity (4–8). This information can then be parsed into *in silico* predicted spectral libraries that can serve as an attractive alternative to empirical spectral libraries.

While DIA for immunopeptidomics is not yet widely adapted, more groups have been exploring this type of acquisition for HLA peptides. For example, DIA has been used for identification of neoantigens (9) or for identification of peptides bound to soluble HLA (10). A significant drawback for use of DIA in immunopeptidomic applications stems from the lack of clear digestion rules for HLA-presented peptides which makes the generation of predicted spectral library a computationally challenging task. Therefore, immunopeptidomics mainly relies on generation of experimental spectral libraries. This is disadvantageous if analyzing samples across multiple cell

From the [1]Department of Proteomic and Genomic Technologies, Genentech Inc, South San Francisco, California, USA; [2]Functional Proteomics, Jena University Hospital, Jena, Germany

*For correspondence: Susan Klaeger, klaeger.susan@gene.com.

https://doi.org/10.1016/j.mcpro.2025.100938

lines or patients with varying HLA types as each of these will present peptides with different binding rules and varying amino acid anchor residues. Moreover, the nonspecific nature of these peptides also complicates data analysis as co-eluting precursors might lead to false identifications.

We have recently shown that ion mobility separation, provided by high field asymmetric waveform ion mobility (Thermo Fisher) (11) or trapped ion mobility spectrometry (TIMS, Bruker Daltonics) (12), helped to increase HLA-I and HLA-II peptide identification starting from more reasonable sample input amounts. Increased sensitivity due to gas phase separation provided by these approaches facilitate detection of substoichiometric posttranslational modifications (13) or neoantigens.

Here, we evaluated the quantitative accuracy of DIA for HLA Class I peptides in combination with ion mobility on the timsTOFscp and proposed an *in silico* library approach using a combination of prediction tools. We then used DIA for identification and quantification of previously identified shared neoantigens in an engineered monoallelic cell line model.

EXPERIMENTAL PROCEDURES

Cell Culture and SILAC Labeling

A375 cells (multiallelic: A*01:01, A*02:01, B*44:03, B*57:01, C*06:02, C*16:01) were cultured in Dulbecco's modified Eagle's medium supplemented with 10% FBS, 2 mM L-glutamine, and 1% penicillin-streptomycin (Gibco). For SILAC experiments, A375 cells were passaged at least seven times in powdered Dulbecco's modified Eagle's medium for SILAC (Thermo Scientific) prepared with either light or heavy amino acid isotopes (84 mg/L L-arginine:HCl [$^{13}C_6$,$^{15}N_4$], 175 mg/L L-lysine:2HCl [$^{13}C_6$,$^{15}N_2$], and 100 mg/L L-leucine [$^{13}C_6$]; Cambridge Isotope Laboratories, Inc.), 44 mM sodium bicarbonate, 10% dialyzed FBS (Thermo Scientific), 200 mg/L L-proline, 2 mM L-glutamine, and 1% penicillin-streptomycin (Gibco). Cells were grown to 90% confluency, harvested with trypsin-EDTA, washed three times with ice cold PBS, and snap frozen.

C1R HLA-A*11:01 monoallelic line containing 47 common cancer mutations was engineered as previously described (Gurung 2023). Briefly, HLA-I null C1R cells were electroporated with a piggyBac neoantigen expression plasmid system and transduced with lentiviral HLA expression vector. Cells were grown in Iscove's Modified Dulbecco's Medium supplemented with 10% FBS and 1ug/ml puromycin (Gibco).

HLA-I Peptide Enrichment and Peptide Elution

A375 cell pellets were lysed in lysis buffer containing 1% CHAPS, 20 mM Tris, pH 8.0, 15 mM NaCl, 2 mM MgCl2, 0.2 mM iodoacetamide, 1 mM EDTA, 1x Complete Protease Inhibitor Tablet-EDTA free, 2 μl benzonase, and 0.2 mM PMSF in total of 2 ml lysis buffer per 100 million cells. Each lysate was incubated on ice for 30 min and vortexed every 5 min. Lysates were then centrifuged at 20,000 rcf for 15 min at 4 °C, and supernatants were transferred to 1 ml 96 deep-well plates. For neoantigen detection, a 500 million cell pellet of a C1R A*11:01 monoallelic cell line containing stably transfected 47-mer cassette without GS linkers was lysed in 5 ml 1% CHAPS lysis buffer, and appropriate volume was taken for the respective dilution point for HLA Class I enrichment.

Immunoprecipitation of HLA-I peptides and sample preclear was performed on AssayMAP Bravo Sample Prep Platform (Agilent), using Affinity Purification v.4 Protocol. Sample preclear was performed by dispensing lysates through 5 μl Protein-A cartridges (Agilent), previously primed and equilibrated with PBS. For enrichment of HLA-I complexes, flow through was loaded on 5 μl W6/32 cross-linked Protein-A cartridges. Cartridges were primed and equilibrated with 100 μl of 20 mM Tris, pH 8.0 and 150 mM NaCl in water. After sample loading, cartridges were washed with 250 μl of 20 mM Tris pH 8.0 and 400 mM NaCl in water followed by final wash with 100 μl of 20 mM Tris pH 8.0 in water. The antibody-bound HLA-peptide complexes were eluted with 60 μl of 0.1 M acetic acid in 0.15% trifluoroacetic acid (TFA) and collected to 96-well PCR, Full Skirt, PolyPro plates (Eppendorf). Two microliter of 30% NH4OH were added to the eluate to neutralize the pH. Samples were then reduced with 5 mM dithiothreitol at 56 °C for 15 min and alkylated with 10 mM iodoacetamide in the dark at RT for 20 min. The samples were then acidified by adding 10% TFA to pH ~ 3.

Next, samples were loaded on the AssayMAP Bravo platform for C18-based desalting. Five microliter C18 cartridges (Agilent) were primed with 80% acetonitrile (ACN) in 0.1% TFA and equilibrated with 0.1% TFA. The samples were afterward loaded through the cartridges, washed with 0.1% TFA, and eluted with 30% ACN in 0.1% TFA and dried by vacuum centrifugation.

LC-MS/MS Analysis

Purified and desalted peptides were reconstituted in 4 μl of solvent A (0.1% formic acid) and separated *via* nanoflow reversed-phase liquid chromatography (Vanquish Neo, Thermo) with 60 min or 120 min methods at flow rate of 0.3 μl/min on an Aurora Ultimate nanoflow UHPLC column with CSI fitting (25 cm × 75 μm ID, 1.7 μm C18, IonOpticks) at 50 °C. Biognosys iRT peptides were spiked into each sample for both DDA and DIA acquisitions. For HLA-A*11:01 dilution DIA runs 100 fmol of previously targeted neoantigens (20) were spiked into the samples. Mobile phase A was H_2O with 0.1 vol% formic acid, and B was ACN with 0.1 vol% formic acid. Peptides eluting from the column were electrosprayed (CaptiveSpray) into a TIMS quadrupole time-of-flight mass spectrometer (Bruker timsTOF SCP). When operated in ddaPASEF, a 10 or three PASEF/MSMS scan per topN acquisition method was utilized. An adapted polygon in the m/z and ion mobility space was employed (12, 14). The mass spectrometer was operated with an accumulation and ramp time of 166 ms or 300 ms. Precursors were isolated with a 2 Th window below m/z 700 and 3 Th above and actively excluded for 0.4 min with a threshold of 10,000 arbitrary units. A range from 100 to 2000 m/z and 0.65 to 1.67 Vs cm-2 was covered with a collision energy 20 eV at 0.6 Vs cm-2 with a linear increase to 59 eV at 1.6 Vs cm-2. When operated in diaPASEF mode, an optimized isolation window scheme in the m/z *versus* ion mobility plane was designed using pydiAID (15), covering >99.5% of all precursor ions including singly charged species. The method covered precursors within 300 to 1200 Da (Table 1). The mass spectrometer was operated in sensitivity mode with an accumulation and ramp time of 100 ms and a cycle time of 1.17 s.

Raw Data Analysis

DDA data were analyzed using FragPipe v20 with a nonspecific HLA workflow, and peptide length was set to 7 to 15 mers against a human database (Uniprot 08/2023, 104,452 protein sequences), including swissprot and trembl entries and 48 common contaminants. Precursor and fragment mass tolerance were both set to 20 ppm. Carbamidomethylation of cysteines was set as static modification, and methionine oxidation, cysteinylation, and pyro-Glu or acetylation of the N terminus were set as variable modification. We allowed a maximum of three variable modifications per peptide. For validation,

TABLE 1
DIA window settings

MSType	CycleId	1/K0Begin[Vs/cm2]	1/K0End[Vs/cm2]	StartMass[m/z]	EndMass[m/z]	CE[eV]	Window
PASEF	1	0.87	1.7	623.75	642.38	-	1.1
PASEF	1	0.4	0.87	300.53	430.23	-	1.2
PASEF	2	0.9	1.7	642.38	662.33	-	2.1
PASEF	2	0.4	0.9	430.23	460.58	-	2.2
PASEF	3	0.91	1.7	662.33	684.36	-	3.1
PASEF	3	0.4	0.91	460.58	481.74	-	3.2
PASEF	4	0.92	1.7	684.36	705.83	-	4.1
PASEF	4	0.4	0.92	481.74	499.26	-	4.2
PASEF	5	0.92	1.7	705.83	727.91	-	5.1
PASEF	5	0.4	0.92	499.26	515.25	-	5.2
PASEF	6	0.93	1.7	727.91	748.92	-	6.1
PASEF	6	0.4	0.93	515.25	529.33	-	6.2
PASEF	7	0.94	1.7	748.92	772.37	-	7.1
PASEF	7	0.4	0.94	529.33	543.28	-	7.2
PASEF	8	0.95	1.7	772.37	801.42	-	8.1
PASEF	8	0.4	0.95	543.28	556.98	-	8.2
PASEF	9	0.96	1.7	801.42	843.91	-	9.1
PASEF	9	0.4	0.96	556.98	573.61	-	9.2
PASEF	10	0.98	1.7	843.91	903.48	-	10.1
PASEF	10	0.4	0.98	573.61	588.32	-	10.2
PASEF	11	1	1.7	903.48	975.48	-	11.1
PASEF	11	0.4	1	588.32	605.41	-	11.2
PASEF	12	1.09	1.7	975.48	1340.62	-	12.1
PASEF	12	0.4	1.09	605.41	623.75	-	12.2

DIA, data-independent acquisition.

MSBooster in combination with Percolator was enabled, and protein false discovery rate (FDR) was disabled. A spectral library was built with the spectral library module in FragPipe using standard parameters and RT alignment to iRT standards (Biognosys).

DIA data were analyzed using DIA-NN, version 1.8.2 beta 11, with standard settings with mass accuracy = 10 p.p.m. and MS1 accuracy = 5 p.p.m., no match between runs, precursor FDR filtering at 1% searching against either sample-specific spectral library, generated by FragPipe, or a predicted library (Table 2).

SILAC DIA data were analyzed with DIA-NN, version 1.8.2 beta 11, with following search settings: Library Generation was set to “IDs, RT and IM Profiling”, Quantification Strategy was set to “Peak height”, Scan window = 1, Mass accuracy = 10 p.p.m., and MS1 accuracy = 5 p.p.m. Additional commands, entered in DIA-NN command window: {–peak-translation}, {–fixed-mod SILAC,0.0,LKR,label}, {–lib-fixed-mod SILAC}, {–channels SILAC,L,LKR,0:0:0; SILAC,H,LKR,6.020 129:8.014199:10.008269}.

Unless otherwise noted, identifications were further filtered for length 8 to 11, tryptic contamination, and contaminants.

HLA Peptide-Binding Prediction

HLA peptide to allele binding was predicted with HLApollo v1 (16). To evaluate MS peptide identifications, identified peptide sequences of length 8 to 13 were evaluated for binding on the cell lines' respective alleles. Peptides were assigned as binders with an HLApollo score >0, and peptides predicted to bind to multiple alleles were assigned to every possible allele. For spectral library generation, all possible 8-13mers from the entire human proteome (swissprot: 62,266 protein sequences, 57,172,493 possible 8–13mer peptides including sequence context for 4 residues at the N and C terminus) were generated and predicted for presentation on A375 cells. Peptides were only retained if they would bind to any of the six alleles with a score >0.

Peptide RT, Fragmentation, and Ion Mobility Prediction with Salud and Ionmob

SaludLibrary (github.com/Genentech/SaludLibrary) was used to create a predicted A375 spectral library (predicted library). HLA peptides identified as binders by HLApollo were considered for charge states 1 to 3 per peptide with fixed cysteine alkylation and variable methionine oxidation as possible modifications. Modified peptides were generated using a function within the python package Pyteomics (17, 18). Within SaludLibrary, spectral features were predicted using Salud, an in-house collection of ML models based on Prosit (7) to predict RT and fragmentation. RT prediction returned a normalized RT that was adjusted for use within the predicted library (library

TABLE 2
Overview of spectral library characteristics

Spectral library name	Cell line	Generation	Number of precursors	Peptide length
Empirical library	A375	Empirical	20,178	7–15
Predicted library	A375	Predicted	382,537	8–13
A1101-combo	C1R - A*11:01	Empirical, plus neoantigen sequences	32,830	7–15

value = [predicted value]*100/2). The peptide fragmentation model was based on the Prosit nontryptic HCD model (19), and the collision energies used for prediction were 15, 20, and 25 for charge states 1, 2, and 3, respectively. The fragmentation model returns an array of intensities for b and y ions (charge states 1–3) that was translated within SaludLibrary to the necessary m/z, z, and intensity values for the predicted library. For ion mobility, collisional cross sections (CCS) were predicted using Ionmob (8), and resulting CCS values were converted to $1/K_0$ values within SaludLibrary. This was accomplished by using ionMob to predict CCS values for a previous data-dependent analysis of HLA peptides and subsequently creating a linear regression between predicted CCS and $1/K_0$ for our particular instrument. We used the resulting equation to convert predicted CCS values for potential binders to $1/K_0$ values for our particular instrument.

Neoantigen Identification and Quantification

In order to systematically identify HLA A*11:01 neoantigens, a two-step approach was used to build a spectral library (A1101-combo) in Fragpipe v20. First, a spectral library was created from all A*11:01 DDA runs using a human proteome fasta file containing the neoantigen sequences along with blue fluorescent protein reporter sequences and iRT sequences (Biognosys). In order to maximize chances of identifying the putative neoantigens, three replicate DDA injections of an equimolar mix of 456 unique synthetic heavy 8-11mer neoantigens that potentially resulted from 47 common cancer mutations (20) were performed as described above using an effective gradient of 51 min. Since the synthetic neoantigen pool contained one heavy amino acid per peptide, mass delta for lysine (K: 8.01499), arginine (R: 10.008269), valine/proline (V/R: 6.0138), leucine/isoleucine (L/I: 7.0171), phenylalanine/tryptophan (F/Y: 10.0272), and alanine (A:4.007) along with methionine oxidation were set as variable modifications. We allowed a maximum of two variable modifications per peptide, and carbamidomethylation of cysteine residue was set as a static modification. We used a fasta file containing only the neoantigen sequences along with blue fluorescent protein reporter sequences and iRT sequences (Biognosys) to build the spectral library containing the heavy peptide sequences. Ion mobility calibration was performed with default selection of *Automatic selection of a run as reference IM*, and only b and y ions were selected for library generation. Following heavy spectral library generation in FragPipe, a custom R script was used to add light labeled transitions to the library for every neoantigen peptide sequence. Then, interference correction was performed by removing identical fragment ion pairs from a combined library of heavy and light neoantigens. Finally, for the library used for searching (A1101-combo), all peptides present in the synthetic peptide library were added to the DDA library, and duplicates were removed. The data were analyzed in DIA-NN, version 1.8.2 beta 11, at 5% precursor FDR by importing the spectral library created with FragPipe v20. Quantification strategy was set as Robust LC (high precision), cross-run normalization as RT-dependent, and library generation as smart profiling. All of the neoantigen identifications by DIA-NN were cross-validated by analyzing them with Skyline (v23.1.0.268) whenever synthetic heavy peptides were available. 100 fmol of each of the previously predicted neoantigens for A*11:01 allele (total 57) were spiked into each dilution sample before data collection. The ratio of endogenous light peptide MS1 area signal to spiked in synthetic heavy was then used to calculate attomole amount for each neoantigen peptide.

Statistical Analysis

All data analysis was performed using custom scripts in python (3.9.4) with packages pandas (1.1.5), numpy (1.22.2), plotly (5.4.0), and scipy (1.7.3) or R (4.3.1) with packages dplyr (1.1.3), data.table (1.14.8), stringr (1.5.1), and ggplot2 (3.4.4). Statistical analysis parameters, if applicable, are described in the respective paragraph and/or figure legend.

Experimental Design and Statistical Rationale

Experiments were performed using A375 cells or engineered C1R cell lines (see respective sections). A375 DIA experiments were performed using three technical replicates. We used the same batch of cultured cells for library creation and DIA injections. Statistical analysis parameters, if applicable, are described in the respective paragraph and/or figure legend. For dilution samples, injections were run from low input to high input to reduce carry over effects.

RESULTS

HLA Peptide Analysis With diaPASEF Workflow

The analytical depth and sensitivity of DIA make it attractive for low-yield samples, such as HLA-peptides. For the initial assessment of a diaPASEF immunopeptidomics workflow, we applied our automated immunoaffinity purification protocol to enrich HLA-I peptides from A375 multiallelic melanoma cells (Fig. 1*A*). In short, we lysed 125 e^6 A375 cells and enriched HLA-I peptides. Peptides from an equivalent of 75 e^6 cells were further split into three replicates, fractionated, and analyzed in DDA mode. To create an experimental DDA-based spectral library, data were analyzed using FragPipe resulting in a final library with 20,178 sequences. The remaining amount was injected in technical quadruplicates (12.5 e^6 cells each) in diaPASEF mode (Fig. 1*B*, supplemental Fig. S1, *A* and *B*) and analyzed by DIA-NN. This led to identification of 10,297 HLA-I peptides from the equivalent of 12.5 e^6 cells in just 60 min of LC gradient time (Fig. 1, *C* and *D*). Notably, we observed a high degree of data completeness with >9500 peptides present in all four replicates (supplemental Fig. S1*C*). Interestingly, >35% of identified peptides are singly charged, which emphasizes the importance of isolation polygon optimization (Fig. 1*E*). Furthermore, all replicates exhibited similar quantitative behavior with a median R^2 of 0.96 and a median coefficient of variation of 12% (Fig. 1*F*). Based on their length distribution and presence of A375 allele-typical anchor residues, we could further verify that identified peptides are indeed HLA-bound with >92% of all identified peptides being 8-13-mers, >70% are predicted to bind to a specific allele, and ~5% could be assigned to multiple alleles in line with observations made for DDA-based experiments (Fig. 1*G*).

DIA Offers High Immunopeptidome Coverage in Half the Analysis Time

We then enriched HLA peptides from reduced cell numbers (500,000–10e^6 A375 cells) in triplicate and found that DIA also increased immunopeptidome coverage when starting with fewer cells (Fig. 2*A*). Notably, DIA identified more precursors than a previously acquired DDA dataset for all cell inputs analyzed using only a 60 min gradient compared to a 120 min gradient for our standard DDA method. Median precursor quantity increased when isolating peptides from a larger number of cells, reflecting the expected abundance changes

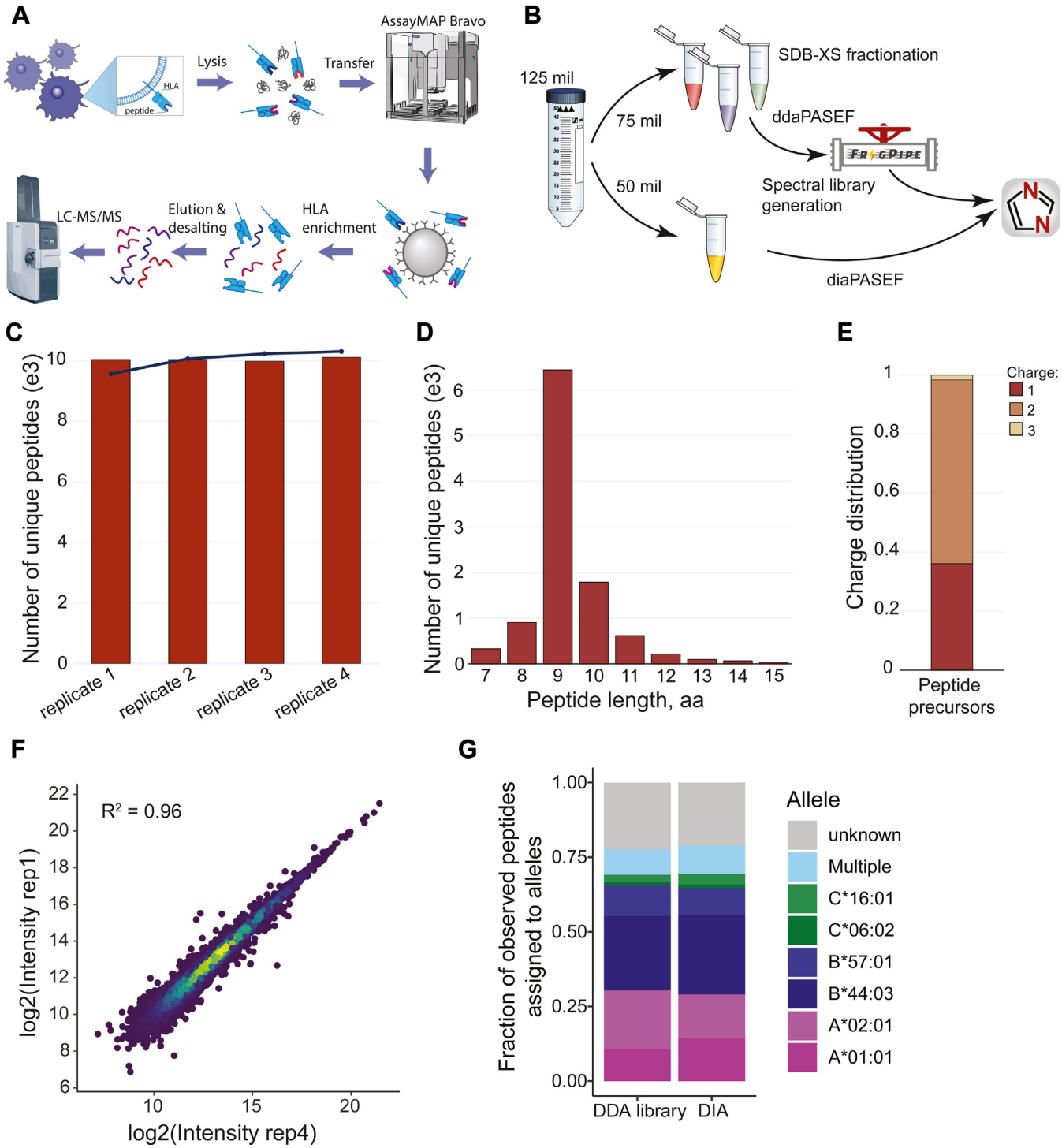

FIG. 1. **diaPASEF identifies HLA peptides with high reproducibility.** *A*, overview of HLA peptide enrichment workflow. *B*, a sample-specific spectral library was created from HLA peptides eluted from 3x 25 e6 cells, fractionated and acquired in ddaPASEF mode. Four replicates were analyzed in diaPASEF mode, and spectra were interpreted using DIA-NN with the sample matched spectral library. *C*, number of unique peptide identifications. *D*, length distribution of peptide IDs. *E*, charge distribution. *F*, intensity correlation between two replicates. *G*, fraction of observed peptides assigned to alleles in DDA library and DIA peptide identifications. DDA, data-dependent acquisition; DIA, data-independent acquisition; HLA, human leukocyte antigen.

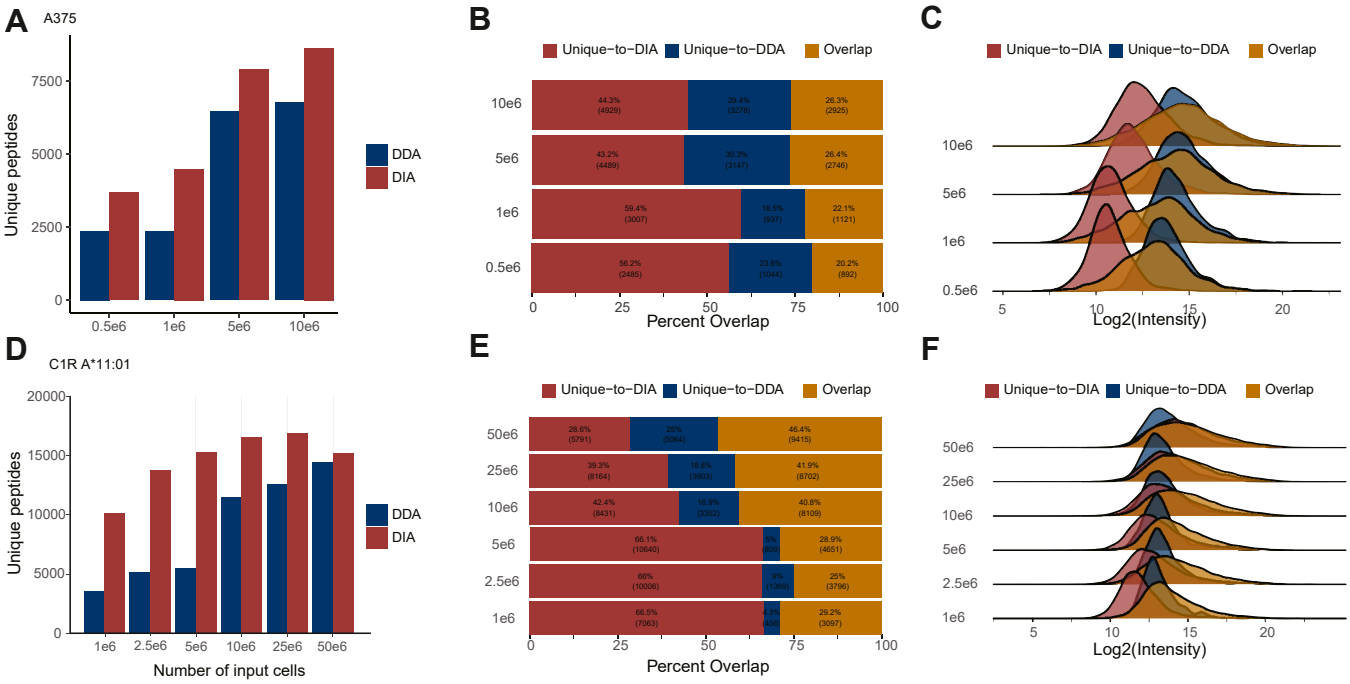

FIG. 2. **DIA outperforms DDA in half the analysis time.** *A*, HLA peptide identifications in DDA and DIA measurements of peptides enriched from decreasing number of A375 cells. *B*, percent overlap of peptide identifications for DDA and DIA for A375. *C*, intensity distribution for precursors identified in both DDA and DIA (overlap) and precursors unique to either acquisition type for A375. *D–F*, same as *A–C* for peptides isolated from C1R cell line monoallelic for HLA-A*11:01. DDA, data-dependent acquisition; DIA, data-independent acquisition; HLA, human leukocyte antigen.

of HLA ligands (supplemental Fig. S2*A*). Furthermore, DIA allowed the identification of >3000 precursors in all conditions (supplemental Fig. S2*B*), while only >1000 peptides were found in all samples with DDA (supplemental Fig. S2*C*), likely due to stochastic intensity-based selection of precursors for MS/MS. For both methods, the majority of peptides are shared between the two higher input conditions (7388 for DIA, 4702 for DDA). We found that the overlap between DDA and DIA identifications for this experiment is 20 to 26% for increasing cell amounts (Fig. 2*B*). Unique DDA identifications were measured with higher intensity values as compared to unique DIA identifications (Fig. 2*C*). These peptides differ slightly in their assigned HLA allele (supplemental Fig. S2*D*), with a slightly larger fraction of unique DDA identifications matching to HLA A*02:01. This can be partially explained by the m/z space of identifications. DDA acquired more singly charged precursors (800–1200 m/z) with higher intensity (supplemental Fig. S2*E*) than DIA, and A*02:01 often produces singly charged precursors. To estimate whether these differences are related to DDA and DIA acquisition at different time points, we performed a similar experiment for peptides isolated from A*11:01 monoallelic cells where DDA and DIA runs, and the spectral library were generated from the same cell lysate and HLA peptide pool. Again, we found that DIA analysis identified more unique peptides compared to DDA (Fig. 2*D*). We observed a larger overlap for DDA and DIA identifications (~30–40%, Fig. 2*E*), and peptide intensity distributions are more similar (Fig. 2*F*) when samples are generated and acquired from the same batch.

Predicted Spectral Features Are a Good Estimate of Empirically Determined Parameters

Experiment-specific spectral libraries facilitate a sensitive matching of HLA peptides acquired with DIA. However, creation of such a library comes at the cost of vast material expenses and typically up to 80% of all available starting material is used to generate a deep experiment-specific spectral library. Alas, often sample-specific libraries have a limited coverage due to low quantity of eluted HLA peptides and inherent disadvantages of the DDA approach. Deep learning algorithms for prediction of MS/MS spectra for existing peptide sequences offer an alternative approach for creation of experiment-specific sample libraries. However, due to the nontryptic nature of HLA peptides, the number of theoretical 8-13-mers from the human proteome exceeds 50 million variants, which complicates directDIA searches.

We, therefore, compared a library containing predicted spectral features of sequences in the library and the empirically generated spectral library. First, to verify the accuracy of RT prediction, we inspected the correlation between predicted RT, calculated by DIA-NN, and measured RT (supplemental Fig. S3, *A* and *B*). Our predicted library showed a slightly higher deviation in comparison with the empirical library that

might point to bigger differences in mean RT prediction between libraries. Indeed, we observed that standard deviation for difference between measured RT and predicted RT in predicted library is ~3-fold higher than in empirical (Fig. 3*A*). However, the difference of DIA-measured RT apex of identified elution profiles between two libraries was within 3 s meaning that both libraries managed to identify the same elution profiles (Fig. 3*B*). We next asked if the predicted spectral library contains sufficient information for quantifying fragment ions in DIA files. Reassuringly, the predicted library yielded a similar fraction of quantified fragment ions hinting on a good quality of fragment intensity predictions by Salud (Fig. 3*C*). Moreover, the overall quality of predictions (median spectral angle = 0.68) was on par with the experiment-specific library (spectral angle = 0.7) (Fig. 3*D*). In concordance with previous studies (9), we found a drop of ~15% in the number of identified HLA peptides with a predicted library in comparison with empirical library (8424 *versus* 10,597). More than 85% of peptides, identified with predicted spectral library, were shared with the empirical one. Interestingly, we found ~15% (1062 peptides) to be found only with predicted library, while 38% of peptides were unique to the empirical library (Fig. 3*E*).

High-Sensitivity Immunopeptidomics With Predicted Libraries

Encouraged by the correlation of empirical and predicted spectral library, we generated a 2-fold prediction strategy to create a synthetic spectral library for A375 that comprised all possible 8-13-mer binders. First, human canonical proteins were predicted for presentation (343,034,958 peptide-HLA allele combinations) using the state of the art predictor HLApollo (16), reducing the possible search space to only 382,537 sequences that could possibly be presented. RT, fragment ions, and ion

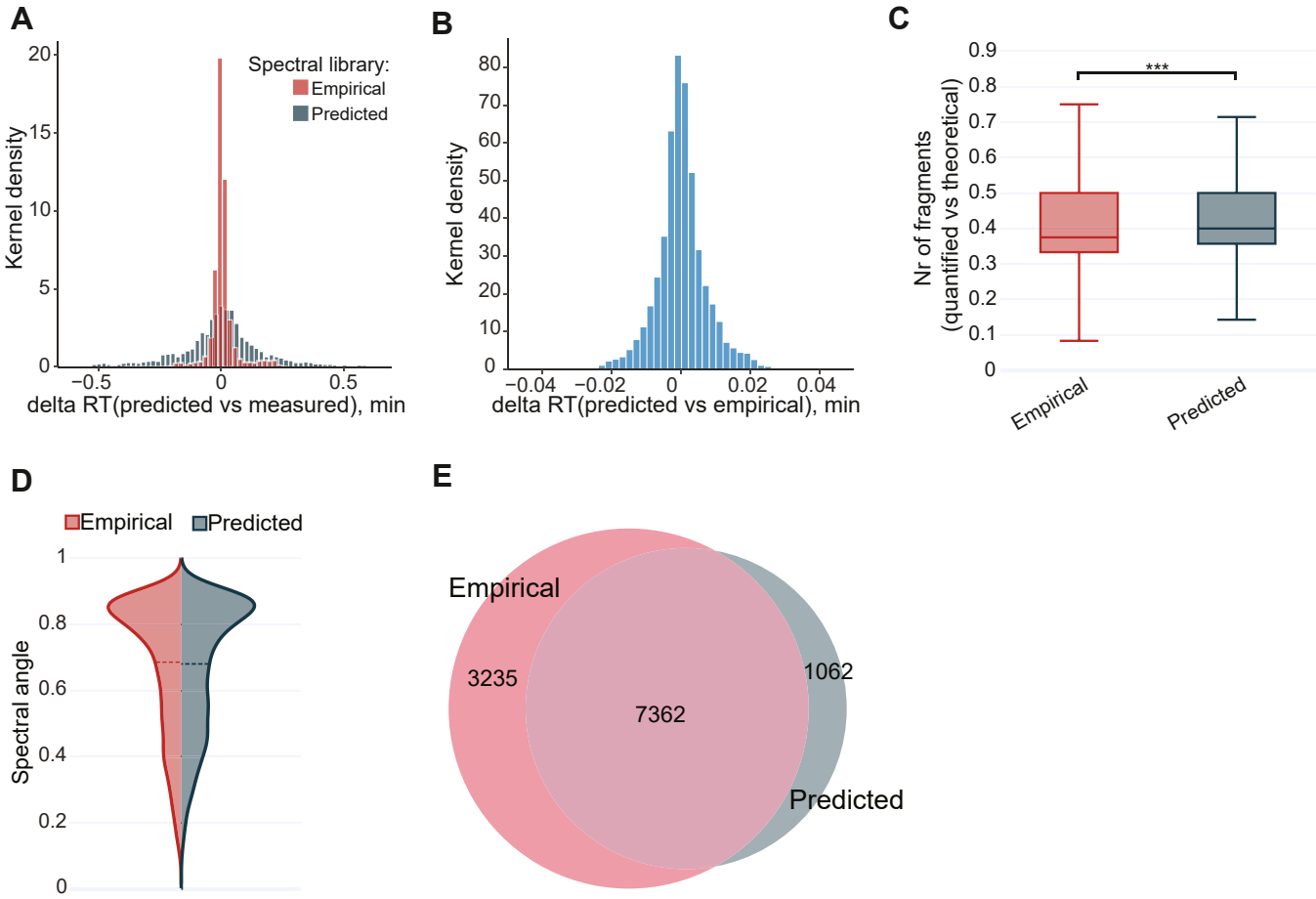

FIG. 3. **Predicted spectral library for HLA peptides can be used to query diaPASEF data.** *A*, comparison of empirically observed retention times to predicted retention times of peptides in the spectral library. *B*, difference of DIA-measured RT apex between both libraries. *C*, ratio of quantified fragment ions compared to available fragment ions in empirical and predicted libraries. *** denotes *p* value < 0.01. *D*, spectral angle of identifications in empirical and predicted libraries. The *dashed line* indicates the median spectral angle. *E*, overlap of identifications when using empirical or predicted libraries. DDA, data-dependent acquisition; DIA, data-independent acquisition; HLA, human leukocyte antigen; RT, retention time.

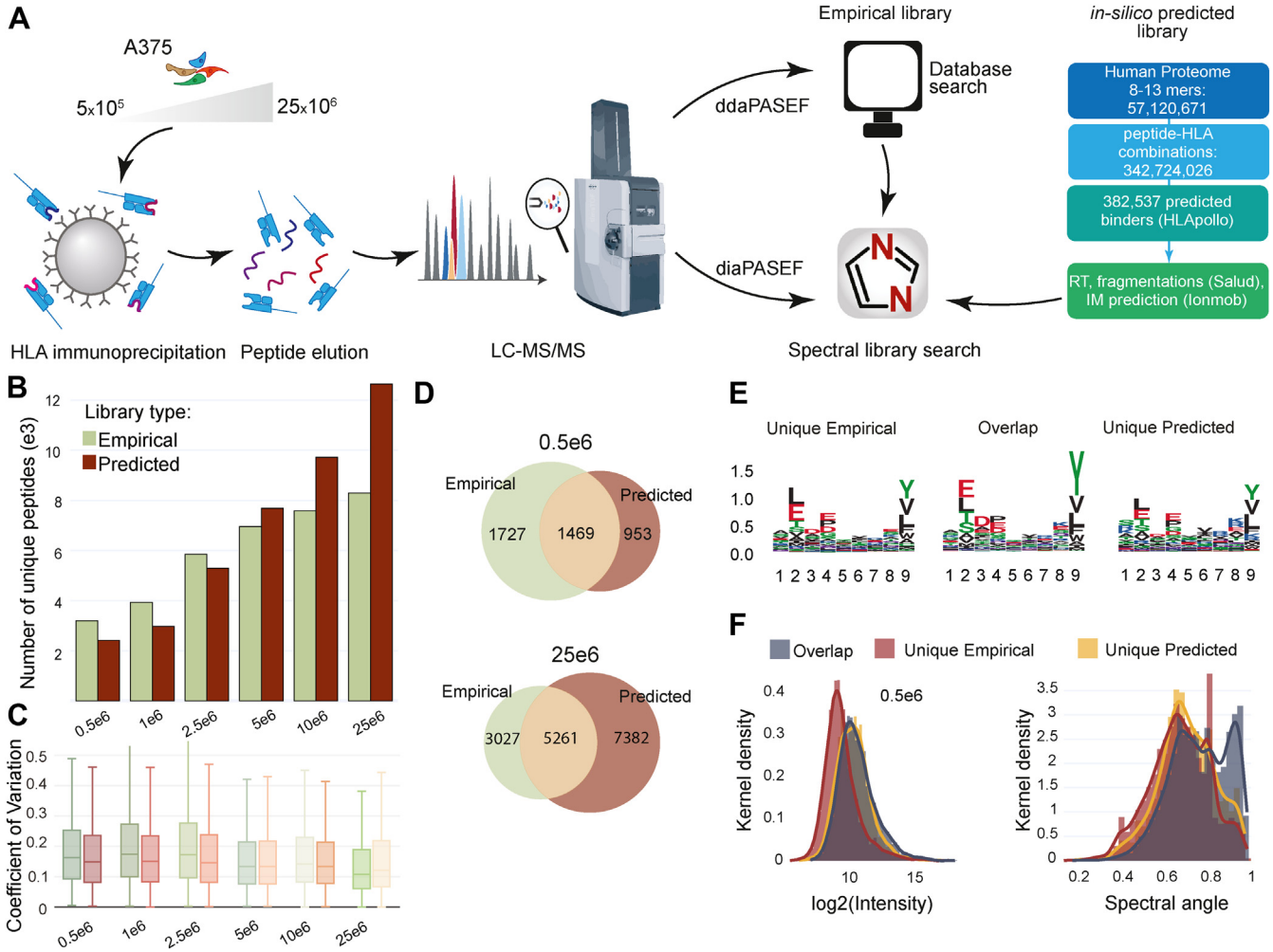

FIG. 4. **Predicted spectral library for all A375 HLA alleles generally outperforms empirical library.** *A*, *in silico* library creation by predicting all possible HLA-peptide combinations for A375 cells and spectral feature prediction with Salud. *B*, number of unique HLA peptides identified with empirical (*green*) or predicted library (*red*). *C*, coefficient of variation of identifications using different spectral libraries. *D*, Venn diagrams of identified peptides for 0.5e6 (*top*) and 25e6 cells (*bottom*). *E*, peptide sequence motifs for identifications overlapping between libraries or uniquely identified with either library. *F*, intensity and spectral angle distribution for identifications overlapping between libraries or uniquely identified with either library for peptides enriched from 0.5e6 cells. HLA, human leukocyte antigen; RT, retention time.

mobility were then predicted for this reduced set of possible precursors using Salud to generate an allele-specific, sample matched spectral library (Fig. 4*A*). Twenty-six percentage of precursors in the empirically generated library were not contained in this predicted library, the majority of those peptides were not predicted to be binders and hence were removed with this proposed approach (supplemental Fig. S4*A*). While we identified slightly more peptides for lower load samples (5e5-2.5e6 cells) with the empirical library, the predicted library was able to identify more peptides for samples enriched from 5e6 to 25e^6 cells, (summarized across triplicates, Fig. 4*B*). Both approaches resulted in high degree of reproducibility with the median coefficient of variation <0.2 across all conditions (Fig. 4*C*). For example, at the 25e6 input level, we identified >12,643 peptides with *in silico* library *versus* ~8288 peptides with the DDA-based library (Fig. 4*D*). While we observed ~35% overlap between libraries, ~42% of peptide IDs found in the empirical library were also identified by the predicted library at 25e^6 input, while at 5e^5 input, ~61% of empirical peptides were also identified with the predicted approach. Interestingly, at an input amount of <5e6 cells, we identified more peptides with the empirical library than in the *in silico* library analysis. However, when comparing motifs of overlapping and unique peptides to either library for the 0.5e6 experiment, we found that all peptides show characteristic sequences for A375 presented peptides (Fig. 4*E*). Upon examination of additional quality criteria such as intensity and spectral angle, peptides identified by the empirical library but not the predicted library show lower intensity and lower spectral angles and might be less confident identifications to begin with (Fig. 4*F*, supplemental Fig. S4, *B* and *C*).

Ion Mobility Reduces Co-Eluting Peptides

Using the predicted spectral features of over 300,000 possibly presented peptides, we further evaluated the ion distribution across DIA windows and LC gradient (supplemental Fig. S5, *A* and *B*, Table 1). Of note, ion mobility already decreased the number of co-eluting precursors per scan from a median of 10 precursors to 1. The majority of predicted precursors fell into windows 1.2 (1/k0:0.4–0.87; m/z: 300.53 mz- 430.23 mz) and window 12.1 (1/k0: 1.09–1.7; m/z: 975.48–1340.62) with >200 precursors eluting in the middle of the LC gradient (supplemental Fig. S5*C*). However, these are deliberately large windows, and not many actual features are observed for these mass/ion mobility combinations. All other DIA window and PASEF cycle combinations contain fewer than 50 precursors that are predicted to be analyzed at a given time in the same window. To characterize the extent of co-fragmentation on HLA peptide sequences, we calculated the occurrence of shared peptide fragments in a PASEF cycle window at a given predicted LC elution point. We compared fragment ions in a wide m/z window and found that many of the predicted, co-eluting ions share fragment ion masses would not be uniquely assigned to a particular peptide unless the ions are of longer length (b/y^9 or higher, supplemental Fig. S5*D*). Reassuringly, this effect is drastically reduced for windows with fewer co-eluting features (such as window 8.2), where only lower m/z fragment ions (<b3/y3) would be shared among co-eluting precursors, and the majority of fragment ions can be uniquely assigned to a single precursor (supplemental Fig. S5*D*). Overall, this analysis shows that the addition of ion mobility significantly reduces the problem of indistinguishable, co-eluting HLA peptides in DIA.

DIA Quantification Benchmarking with SILAC

Next, we derived a SILAC HLA peptide DIA strategy to evaluate quantitative accuracy and precision. A375 cells grown in heavy SILAC (K, R, L) and light medium were mixed to a total of $20e^6$ cells each at ratios 1:1, 1:2, 1:4, 1:9, and 1:19 prior to lysis, HLA peptide enrichment, and DIA (Fig. 5*A*). DIA data were analyzed using an A375 spectral library and DIA-NN with SILAC-specific parameters (Methods). Not all presented peptides contained an amino acid used in the SILAC mix. Therefore, H/L ratios could be calculated for 70 to 80% of peptides identified in each experiment. Median H/L ratios for all peptides identified per sample closely matched expected H/L ratios for 1:1, 1:2, and 1:4 dilutions with only 0 to 4% relative error (Fig. 5*B*). For dilutions 1:9 and 1:19, measured ratios had 16% or 46% relative error compared to the expected ratio. This is likely due to identification of lower intensity precursors, mis-identifying light labeled peptides as heavy labeled and vice versa (supplemental Fig. S6*A*). Indeed, when examining the quality of the spectral match, heavy identifications have a greater C-Score distribution than light labeled peptide identifications, with a median of 0.5 C-score for heavy peptides in the 1:19 dilution (supplemental Fig. S6*B*). However, while additional filtering for channel and translated q values (21) improved C-scores of remaining peptides (supplemental Fig. S6*C*), it did not affect median ratio or remove peptides with extreme ratios (supplemental Fig. S6*D*). This indicates that peptides are either mis-identified or suffer from high signal to noise at extreme ratios and need to be evaluated carefully. Overall, quantitation is accurate up to 5-fold dilution, in line with similar studies on low input samples (22).

Identification and Quantification of Common Cancer Neoantigens

Next, we evaluated how DIA analysis could benefit neoantigen identification and quantification. We used a mono-allelic C1R cell line expressing HLA-A*11:01 that was transfected with a neoantigen cassette encoding 47 common cancer mutations (Fig. 6*A*) (20). HLA complexes were enriched from $1e^6$ to $50e^6$ cells and eluted, followed by DDA for library generation and then DIA. Prior to DIA analysis, 100 fmol of synthetic, heavy standard peptides were spiked into the

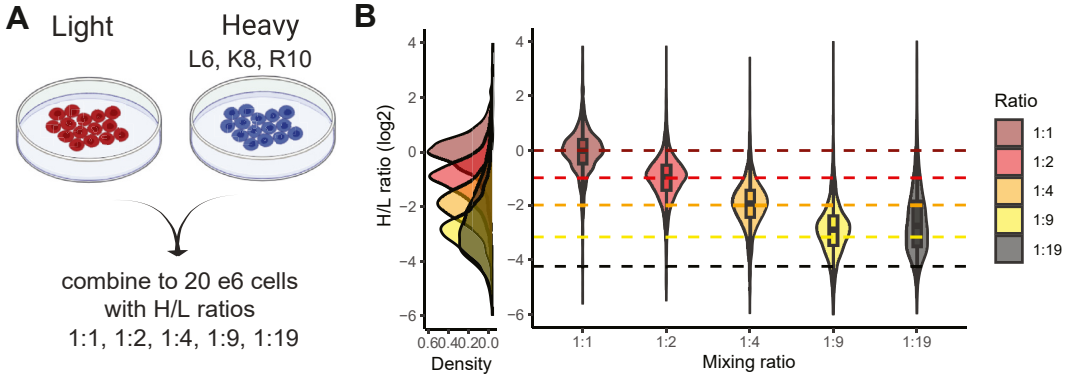

FIG. 5. **diaPASEF quantification benchmarking with SILAC.** *A*, SILAC labeling strategy for HLA peptide analysis. *B*, violin and density plot for log2 H/L ratios across mixing ratio experiments. Box plots show median ratio, and dotted lines indicate expected ratio. HLA, human leukocyte antigen.

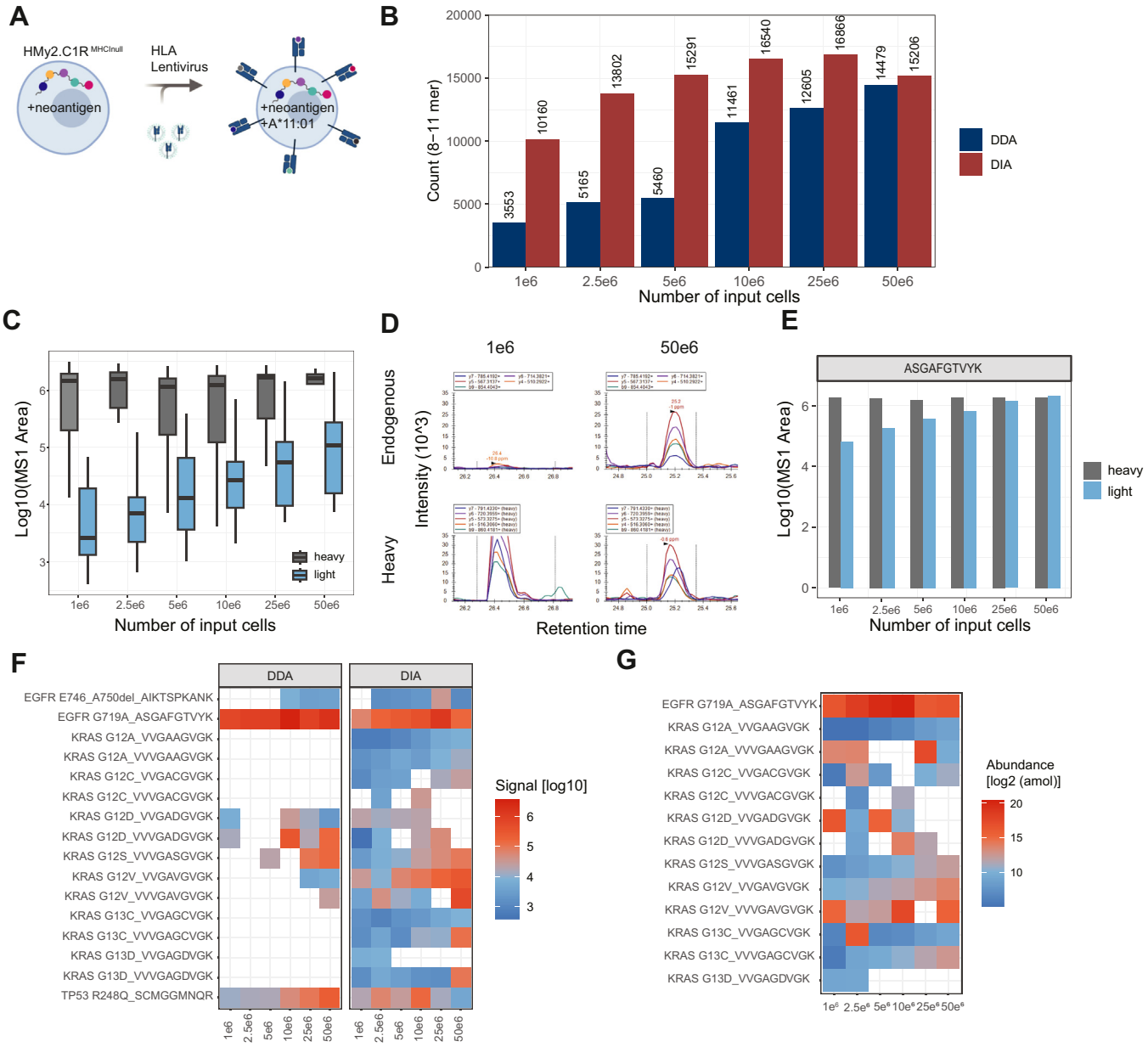

FIG. 6. **diaPASEF identification and quantification of A*11:01 neoantigens.** *A*, HLA-I-null C1R cell lines were transfected with a neoantigen cassette containing 47 common cancer mutations and an HLA-I allele of interest, and HLA ligands were eluted from increasing cell amounts. *B*, HLA peptide identifications in DDA and DIA measurements of peptides enriched from increasing cell amounts. *C*, MS1 area of endogenous presented peptides increased while synthetic spike in areas were stable. *D*, extracted Ion Chromatograms (XIC) of endogenous (*top*) and heavy labeled neoantigen peptides. *E*, same as D but quantified using DIA-NN MS1 area. *F*, intensity of neoantigen identifications in DDA and DIA acquisition increases with increasing sample input. *G*, abundance of all neoantigens identified and quantified by DIA in A*11:01 C1R cells normalized to 100 fmol of heavy synthetic spike in peptides. DDA, data-dependent acquisition; HLA, human leukocyte antigen; DIA, data-independent acquisition.

sample. This allowed for an internal control and helped eliminate false positive identification as spiked in peptides co-elute and co-fragment. We observed a steady increase in identifications up to 10e6 and 25e6 cells. Interestingly, identifications decreased for 50e6 cells in DIA runs compared to DDA, likely due to space charging, gradient, or library constraints (Fig. 6*B*). We observed an increase in abundance of neoantigens while the spike-in MS1 area stayed relatively constant (Fig. 6*C*). For example, while a neoantigen from EGFR G719 A was low abundant at 1e6 cell input, it could be detected across all input ranges tested with increasing presentation on the surface (Fig. 6, *D* and *E*). We identified 16

peptide sequences from the neoantigen construct, the majority of sequences from KRAS mutant sequences. As expected, DIA provided a more complete coverage across the dilution series and detected 14/16 neoantigens in as low as 1e6 cell input (Fig. 6*F*). Using the signal of heavy spike-in peptides, we quantified the relative abundance of 13 neoantigens on the surface starting at 33 attomoles for 1e6 cells (Fig. 6*G*). For comparison, 20 neoantigens were found in a targeted PRM experiment and nine with DDA from 166e6 cells (20). This highlights the general utility of DIA acquisition for quantification in immunopeptidomics experiments when following selected peptides of interest across samples.

Collectively, these results point to high analytical depth and exceptional quantitative reproducibility of DIA in the context of immunopeptidomics.

DISCUSSION

Advancements in instrumentation have further increased the application of DIA in numerous proteomic studies. Key advantages include reproducibility between replicates and relative quantification across a large number of samples. For DDA-based immunopeptidomic measurements, reproducibility between replicates historically ranges between 60 and 70%. With DIA, we achieved over 99% overlap of identified peptides in replicates. The integration of ion mobility, such as field asymmetric waveform ion mobility or TIMS, decreases the number of co-eluting precursors, and fewer overlapping or shared fragment ions allow for higher confidence in identifications.

Though DIA resulted in great depth of coverage with reduced acquisition time of an immunopeptidome sample of interest, additional sample material is needed to create a spectral library. Due to the biological complexity of HLA peptidome samples, library-based approaches are necessary to keep FDR low. Other studies have predicted a smaller set of peptides of interest to be included in a spectral library or generated a large library of available public HLA peptide data on either sequence or spectral level independent of sample context and HLA types present in a sample (9, 10). We propose a two-step strategy that first employs state-of-the-art HLA binding predictors to reduce the possible number of peptide sequences in the human proteome and tailor them to the sample of investigation. The second step includes the prediction of spectral features similar to published approaches. This combined prediction approach leads to similar or more identifications depending on the amount of peptide loaded on column. Of note, such a predicted library is highly dependent on the prediction algorithm used and might miss novel peptide sequences not included in the binding prediction or sequences predicted as nonbinders. It can be further refined by adding contaminant species and noncanonical peptide sequences. Prediction results can also be used to filter peptides further, for example, peptides uniquely identified in experimentally determined spectral libraries are of lower intensity and show poorer spectral angle, indicating that these might be lower confidence hits.

Using all possible presented precursors, we could also evaluate our data acquisition approach. We found that ion mobility in general reduces the number of co-eluting and co-fragmenting peptides and even for highly similar peptide sequences like HLA-presented peptides, most DIA spectra contain <50 features with distinct fragment ions. Additional data acquisition approaches further improving window design, as well as novel approaches such as sliceDIA or synchroPASEF (23, 24), midiaPASEF (25), and narrow window acquisition (26), can further decrease co-elution and cofragmentation leading to confident identifications.

DIA acquisition is quite powerful for quantification across many samples compared to DDA-based label-free or TMT-based quantification. For instance, assessing peptide abundance changes due to varying treatment conditions or input amounts in a consistent sample background is likely executed more efficiently with DIA. But due to the inherent diversity of the HLA peptidome, stratification by respective HLA types is pivotal before conducting such experiments. We evaluated quantitative accuracy using a SILAC approach and found that DIA analysis can accurately recover known quantities up to a 5-fold difference. Quantification of larger ratios suffers from background noise contamination or incomplete fragmentation and wrong assignment of spectral matches. This is in line with reports in other studies including single cell analyses (22, 27). In cell line samples carrying common tumor mutations, we were able to detect neoantigen peptides in as low as 1e6 cells input into the immunoprecipitation and quantify increasing amounts of peptides with increasing amounts of cells. If coupled with a heavy isotope-labeled-major histocompatibility complex approach (28), ratios of light to heavy peptides can be used to determine the copy number of peptides presented on the surface, while still gathering data on all other peptides present in the sample and hence not losing additional peptidome information discarded in PRM acquisitions (29, 30).

Collectively, the integration of DIA with ion mobility emerges as a potent data acquisition approach. It enhances reproducibility and facilitates effortless quantification of peptides within the same HLA allele-type background. Additionally, the library-free strategy we proposed for HLA immunopeptidome measurements can be conveniently constructed using existing resources. This approach, coupled with DIA measurements, ensures robust quantification which can significantly increase throughput, proving advantageous to studies appraising immunotherapy mode of action.

DATA AVAILABILITY

The original mass spectra, peptide reports, and spectral libraries have been deposited in the public proteomics repository MassIVE (https://massive.ucsd.edu) with the associated MSV identifier MSV000095137 and can be

accessed at ftp://massive.ucsd.edu/v08/MSV000095137/. SaludLibrary source code can be found at github.com/Genentech/SaludLibrary, and the version used for this publication has been deposited at Zenodo (https://doi.org/10.5281/zenodo.14908088).

Supplemental Data—This article contains supplemental data.

Acknowledgments—The authors want to thank Felipe da Veiga Leprevost, Meena Choi, and Alessandro Ori for insightful discussions.

Author contribution—D. O., H. R. G., K. L., and C. M. R. investigation; Z. Z. and C. M. R. software; D. O., H. R. G., Z. Z., C. M. R., and S. K. methodology; H. R. G. and S. K. writing–review and editing; D. O., H. R. G., and S. K. writing–original draft; D. O., H. R. G., and S. K. visualization; D. O., H. R. G., and S. K. formal analysis; D. O., H. R. G., and S. K. data curation; S. K. supervision; S. K. resources; S. K. project administration; D. O., H. R. G., C. M. R., and S. K. conceptualization.

Conflict of interest—All authors were employees of Genentech Inc. at the time of performing the research and writing the manuscript; H. G., K. L., Z. Z., C. M. R., and S. K. are shareholders of Roche. The authors declare that they have filed a patent application related to the technology/methods described in this article.

Abbreviations—The abbreviations used are: ACN, acetonitrile; CCS, collisional cross sections; DDA, data-dependent acquisition; DIA, data-independent acquisition; FDR, false discovery rate; HLA, human leukocyte antigen; MS, mass spectrometry; RT, retention; TFA, trifluoroacetic acid; TIMS, trapped ion mobility spectrometry.

Received July 30, 2024, and in revised form, February 24, 2025
Published, MCPRO Papers in Press, March 3, 2025, https://doi.org/10.1016/j.mcpro.2025.100938

REFERENCES

1. Yewdell, J. W. (2022) MHC class I immunopeptidome: past, present & future. *Mol. Cell Proteom Mcp* **21**, 100230
2. Bassani-Sternberg, M., Bräunlein, E., Klar, R., Engleitner, T., Sinitcyn, P., Audehm, S., *et al*. (2016) Direct identification of clinically relevant neoepitopes presented on native human melanoma tissue by mass spectrometry. *Nat. Commun.* **7**, 13404
3. Yadav, M., Jhunjhunwala, S., Phung, Q. T., Lupardus, P., Tanguay, J., Bumbaca, S., *et al*. (2014) Predicting immunogenic tumour mutations by combining mass spectrometry and exome sequencing. *Nature* **515**, 572–576
4. Adams, C., Gabriel, W., Laukens, K., Picciani, M., Wilhelm, M., Bittremieux, W., *et al*. (2024) Fragment ion intensity prediction improves the identification rate of non-tryptic peptides in TimsTOF. *Nat. Commun.* **15**, 3956
5. Bouwmeester, R., Gabriels, R., Hulstaert, N., Martens, L., and Degroeve, S. (2021) DeepLC can predict retention times for peptides that carry as-yet unseen modifications. *Nat. Methods* **18**, 1363–1369
6. Declercq, A., Bouwmeester, R., Hirschler, A., Carapito, C., Degroeve, S., Martens, L., *et al*. (2022) MS2Rescore: data-driven rescoring dramatically boosts immunopeptide identification rates. *Mol. Cell Proteomics* **21**, 100266
7. Gessulat, S., Schmidt, T., Zolg, D. P., Samaras, P., Schnatbaum, K., Zerweck, J., *et al*. (2019) Prosit: proteome-wide prediction of peptide tandem mass spectra by deep learning. *Nat. Methods* **16**, 509–518
8. Teschner, D., Gomez-Zepeda, D., Declercq, A., Łącki, M. K., Avci, S., Bob, K., *et al*. (2023) Ionmob: a Python package for prediction of peptide collisional cross-section values. *Bioinformatics* **39**, btad486
9. Pak, H., Michaux, J., Huber, F., Chong, C., Stevenson, B. J., Müller, M., *et al*. (2021) Sensitive immunopeptidomics by leveraging available large-scale multi-HLA spectral libraries, data-independent acquisition, and MS/MS prediction. *Mol. Cell Proteomics* **20**, 100080
10. Wahle, M., Thielert, M., Zwiebel, M., Skowronek, P., Zeng, W.-F., and Mann, M. (2024) IMBAS-MS discovers organ-specific HLA peptide patterns in plasma. *Mol. Cell. Proteom.* **23**, 100689
11. Klaeger, S., Apffel, A., Clauser, K. R., Sarkizova, S., Oliveira, G., Rachimi, S., *et al*. (2021) Optimized liquid and gas phase fractionation increases HLA-peptidome coverage for primary cell and tissue samples. *Mol. Cell Proteom Mcp* **20**, 100133
12. Phulphagar, K. M., Ctortecka, C., Jacome, A. S. V., Klaeger, S., Verzani, E. K., Hernandez, G. M., *et al*. (2023) Sensitive, high-throughput HLA-I and HLA-II immunopeptidomics using parallel accumulation-serial fragmentation mass spectrometry. *Mol. Cell. Proteom* **22**, 100563
13. Oliinyk, D., and Meier, F. (2022) Ion mobility-resolved phosphoproteomics with dia-PASEF and short gradients. *Proteomics* **23**, 2200032
14. Gomez-Zepeda, D., Arnold-Schild, D., Beyrle, J., Declercq, A., Gabriels, R., Kumm, E., *et al*. (2024) Thunder-DDA-PASEF enables high-coverage immunopeptidomics and is boosted by MS2Rescore with MS2PIP timsTOF fragmentation prediction model. *Nat. Commun.* **15**, 2288
15. Skowronek, P., Thielert, M., Voytik, E., Tanzer, M. C., Hansen, F. M., Willems, S., *et al*. (2022) Rapid and in-depth coverage of the (Phospho-) Proteome with deep libraries and optimal window design for dia-PASEF. *Mol. Cell. Proteom.* **21**, 100279
16. Thrift, W. J., Lounsbury, N. W., Broadwell, Q., Heidersbach, A., Freund, E., Abdolazimi, Y., *et al*. (2024) Towards designing improved cancer immunotherapy targets with a peptide-MHC-I presentation model, HLApollo. *Nat. Commun.* **15**, 10752
17. Levitsky, L. I., Klein, J. A., Ivanov, M. V., and Gorshkov, M. V. (2019) Pyteomics 4.0: five years of development of a Python proteomics framework. *J. Proteome Res.* **18**, 709–714
18. Goloborodko, A. A., Levitsky, L. I., Ivanov, M. V., and Gorshkov, M. V. (2013) Pyteomics—a Python framework for exploratory data analysis and rapid software prototyping in proteomics. *J. Am. Soc. Mass Spectrom.* **24**, 301–304
19. Wilhelm, M., Zolg, D. P., Graber, M., Gessulat, S., Schmidt, T., Schnatbaum, K., *et al*. (2021) Deep learning boosts sensitivity of mass spectrometry-based immunopeptidomics. *Nat. Commun.* **12**, 3346
20. Gurung, H. R., Heidersbach, A. J., Darwish, M., Chan, P. P. F., Li, J., Beresini, M., *et al*. (2023) Systematic discovery of neoepitope–HLA pairs for neoantigens shared among patients and tumor types. *Nat. Biotechnol.* **42**, 1107–1117
21. Borteçen, T., Müller, T., and Krijgsveld, J. (2023) An integrated workflow for quantitative analysis of the newly synthesized proteome. *Nat. Commun.* **14**, 8237
22. Petrosius, V., Aragon-Fernandez, P., Üresin, N., Kovacs, G., Phlairaharn, T., Furtwängler, B., *et al*. (2023) Exploration of cell state heterogeneity using single-cell proteomics through sensitivity-tailored data-independent acquisition. *Nat. Commun.* **14**, 5910
23. Skowronek, P., Krohs, F., Lubeck, M., Wallmann, G., Itang, E. C. M., Koval, P., *et al*. (2023) Synchro-PASEF allows precursor-specific fragment ion extraction and interference removal in data-independent acquisition. *Mol. Cell Proteomics* **22**, 100489
24. [preprint] Szyrwiel, L., Sinn, L., Ralser, M., and Demichev, V. (2022) Slice-PASEF: fragmenting all ions for maximum sensitivity in proteomics. *bioRxiv*. https://doi.org/10.1101/2022.10.31.514544
25. [preprint] Distler, U., Lacki, M. K., Startek, M. P., Teschner, D., Brehmer, S., Decker, J., *et al*. (2023) midiaPASEF maximizes information content in data-independent acquisition proteomics. *bioRxiv*. https://doi.org/10.1101/2023.01.30.526204

26. Guzman, U. H., Martinez-Val, A., Ye, Z., Damoc, E., Arrey, T. N., Pashkova, A., *et al*. (2024) Ultra-fast label-free quantification and comprehensive proteome coverage with narrow-window data-independent acquisition. *Nat. Biotechnol.* **42**, 1855–1866
27. Pino, L. K., Baeza, J., Lauman, R., Schilling, B., and Garcia, B. A. (2021) Improved SILAC quantification with data-independent acquisition to investigate bortezomib-induced protein degradation. *J. Proteome Res.* **20**, 1918–1927
28. Stopfer, L. E., Gajadhar, A. S., Patel, B., Gallien, S., Frederick, D. T., Boland, G. M., *et al*. (2021) Absolute quantification of tumor antigens using embedded MHC-I isotopologue calibrants. *Proc. Natl. Acad. Sci.* **118**, e2111173118
29. Martínez-Val, A., Fort, K., Koenig, C., Hoeven, L. V. der, Franciosa, G., Moehring, T., *et al*. (2023) Hybrid-DIA: intelligent data acquisition integrates targeted and discovery proteomics to analyze phosphosignaling in single spheroids. *Nat. Commun.* **14**, 3599
30. Goetze, S., Drogen, A. van, Albinus, J. B., Fort, K. L., Gandhi, T., Robbiani, D., *et al*. (2024) Simultaneous targeted and discovery-driven clinical proteotyping using hybrid-PRM/DIA. *Clin. Proteom.* **21**, 26